

Importance of N₂ fixation vs. nitrate eddy diffusion along a latitudinal transect in the Atlantic Ocean

Beatriz Mouriño-Carballido,^{a,*} Rocío Graña,^b Ana Fernández,^a Antonio Bode,^c Manuel Varela,^c J. Francisco Domínguez,^d José Escáñez,^d Demetrio de Armas,^d and Emilio Marañón^a

^aDepartamento de Ecología y Biología Animal, Universidad de Vigo, Vigo, Spain

^bDepartamento de Física Aplicada, Universidad de Vigo, Vigo, Spain

^cInstituto Español de Oceanografía, Centro Oceanográfico de A Coruña, A Coruña, Spain

^dInstituto Español de Oceanografía, Centro Oceanográfico de Canarias, Santa Cruz de Tenerife, Spain

Abstract

We present ocean, basin-scale simultaneous measurements of N₂-fixation, nitrate diffusion, and primary production along a south–north transect in the Atlantic Ocean crossing three biogeographic provinces: the south subtropical Atlantic (SSA; ~ 31°S–12°S), the equatorial Atlantic (EA; ~ 12°S–16°N), and the north subtropical Atlantic (NSA, ~ 16°N–9°N) in April–May 2008. N₂-fixation and primary production were measured as ¹⁵N₂ and ¹⁴C uptake, respectively. Dissipation rates of turbulent kinetic energy (ϵ) were measured with a microstructure profiler. The vertical input of nitrate through eddy diffusion was calculated from the product of diffusivity, derived from ϵ , and the gradient of nanomolar nitrate concentration across the base of the euphotic zone. The mean N₂-fixation rate in EA was $56 \pm 49 \mu\text{mol N m}^{-2} \text{d}^{-1}$, whereas SSA and NSA had much lower values ($\sim 10 \mu\text{mol N m}^{-2} \text{d}^{-1}$). Because of the large spatial variability in nitrate diffusion (34 ± 50 , 405 ± 888 , and $844 \pm 1258 \mu\text{mol N m}^{-2} \text{d}^{-1}$ in SSA, EA, and NSA, respectively), the contribution of N₂-fixation to new production in the SSA, EA, and NSA was $44\% \pm 30\%$, $22\% \pm 19\%$, and $2\% \pm 2\%$, respectively. The differences between SSA and NSA in the contribution of N₂ fixation were partly due to the contrasting seasonal forcing in each hemisphere, which likely affected both N₂ fixation rates and vertical nitrate diffusion. The variability in the nitrogen budget of the Atlantic subtropical gyres was unexpectedly high and largely uncoupled from relatively constant phytoplankton standing stocks and primary production rates.

Nitrogen has a critical role in controlling primary production in both marine and land ecosystems (Falkowski 1997). Assuming steady state in the euphotic zone, new production (the input of new nitrogen into the euphotic layer of the ocean) constrains the potential of the biological pump for organic carbon export to deeper layers and net sequestration of atmospheric CO₂ in the ocean's interior (Eppley and Peterson 1979).

In the warm tropical and subtropical ocean, phytoplankton biomass is low due to the scarcity of nutrients caused by strong water stratification. Despite their low phytoplankton biomass, these regions cover a large surface, which results in their contribution of up to 30% of the global export of biogenic carbon into the deep ocean (Emerson et al. 1997; Najjar et al. 2007). In these regions, nitrogen supply to the euphotic layer occurs through a variety of mechanisms including diffusion across the thermocline, mesoscale, and submesoscale turbulence (Oschlies and Garçon 1998), lateral transport of organic and inorganic nutrients from the surrounding productive regions (Williams and Follows 1998; Torres-Valdes et al. 2009), atmospheric deposition (Duce et al. 2008), and nitrogen fixation (Moore et al. 2009). Although nitrate diffusion has traditionally been considered the dominant mechanism, recent studies indicate that N₂ fixation could equal or even exceed the vertical input of nitrate (Capone et al. 2005). However, these two fluxes have never been

measured concurrently and, thus, their magnitude, variability, and relative importance remain poorly known.

Previous attempts to assess the relative importance of N₂ fixation vs. nitrate eddy diffusion in supporting new production have assumed constant diffusivity (k_z) across the thermocline (Capone et al. 2005). Yet, the magnitude and distribution of diffusivity in the ocean interior is not well-constrained. Measurements of dissipation rates of turbulence kinetic energy (Lewis et al. 1986) and tracer release experiments (Ledwell et al. 1993) indicate that mixing in the thermocline is about $10^{-5} \text{m}^2 \text{s}^{-1}$. This value is one order of magnitude lower than those inferred from budget analyses (Munk 1966). It has been proposed that this mismatch could result from constraints of traditional sampling studies that very often miss episodic hot spots of turbulent mixing. In this regard, vertical diffusivity computed by comparing surface temperatures before and after tropical storm passage indicated that tropical cyclones are responsible for significant cooling and vertical mixing of the surface ocean (Srifer and Huber 2007). Recently, Katija and Dabiri (2009) provided new evidence for the role of biologically generated turbulence. A recent compilation of k_z values ranged from $10^{-4} \text{m}^2 \text{s}^{-1}$ to $10^{-1} \text{m}^2 \text{s}^{-1}$ (Wunsch and Ferrari 2004). Doubts about the underlying theoretical assumptions to derive k_z from the observations, and about the extent to which the few available k_z values are representative of large open-ocean regions, justify further efforts to obtain direct measurements of diffusivity.

* Corresponding author: bmourino@uvigo.es

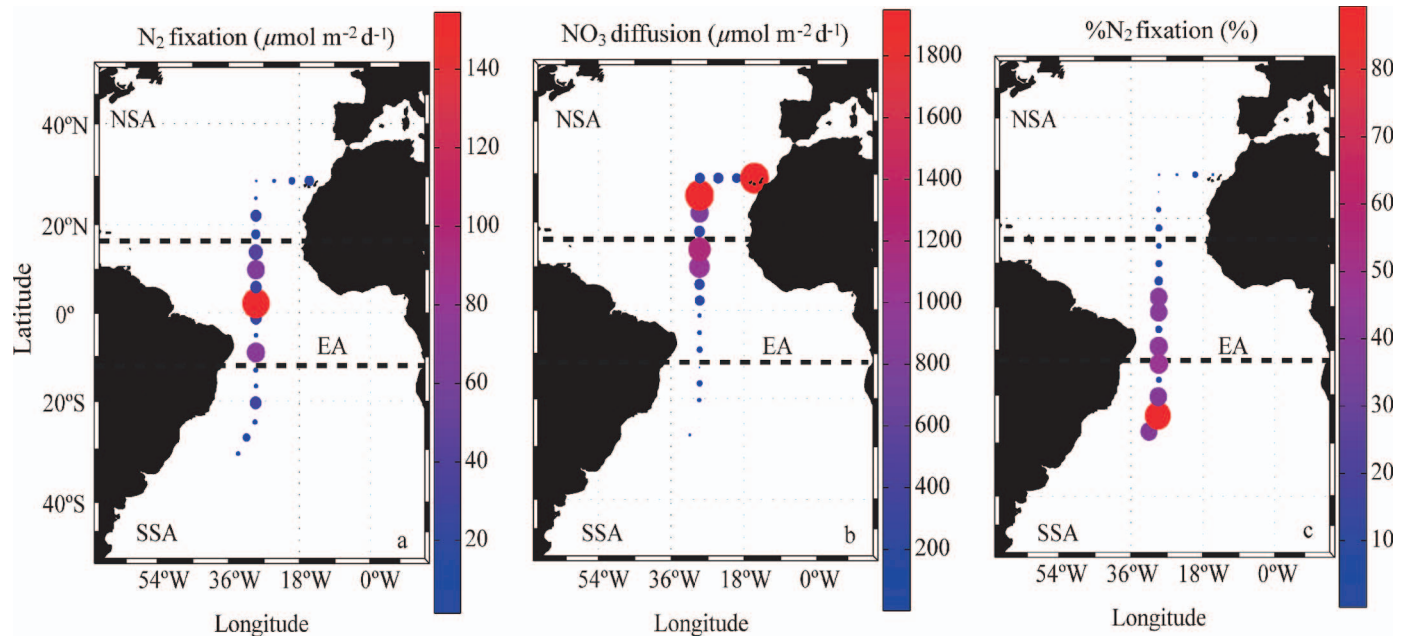


Fig. 1. Distribution of (a) N_2 fixation rates integrated down to the base of the euphotic zone ($\mu\text{mol m}^{-2} \text{d}^{-1}$), (b) vertical flux of nitrate entering the euphotic zone through eddy diffusion ($\mu\text{mol m}^{-2} \text{d}^{-1}$), and (c) contribution (%) of N_2 fixation to total new nitrogen input during this cruise. The cruise track crossed the south subtropical Atlantic (SSA; $\sim 31^\circ\text{S}$ – 12°S), the equatorial Atlantic (EA; $\sim 12^\circ\text{S}$ – 16°N), and the north subtropical Atlantic (NSA; $\sim 16^\circ\text{N}$ – 29°N). Bubbles size is proportional to the magnitude of the represented variable.

Here we present the first basin-scale, simultaneous measurements of N_2 fixation, nitrate eddy diffusion, and primary production in the open ocean. Our main goal was to determine the large-scale spatial variability in the importance of N_2 fixation vs. nitrate diffusion as a source of new nitrogen in the Atlantic Ocean.

Methods

Field observations were carried out in the Atlantic Ocean along a transect from 30°S to 30°N during 14 April–02 May 2008 (see Fig. 1) during the TRYNITROP (*Trichodesmium* and N_2 fixation in the Atlantic Ocean) cruise. Twenty-eight conductivity temperature depth (CTD) stations were conducted with a SBE911plus probe (Sea-Bird Electronics) attached to a rosette equipped with Niskin bottles. During this cruise and a previous cruise conducted along the same track, in October–November 2007 (Fernández et al. 2010), 16 vertical profiles of photosynthetically active irradiance (PAR; 400–700 nm) were obtained at noon with a Satlantic Ocean Color Profiler 100FF radiometer. A highly significant relationship was obtained between the depth of the 1% PAR (Z_{eu}) and the depth of the deep chlorophyll maximum identified by in situ fluorescence (ZDCM): $Z_{\text{eu}} = 9.3 + 0.98 \times \text{ZDCM}$ ($r^2 = 0.93$, $p < 0.001$, $n = 16$). This relationship was used to estimate the depth of the euphotic zone in those stations where PAR information was not available. Samples were collected on each CTD cast conducted at dawn for the determination of dissolved inorganic nitrogen, chlorophyll *a* (Chl *a*), and primary production, as well as for the measurement of N_2 fixation rates. The concentration of

nitrate, nitrite, and ammonium, was determined on board on fresh samples with a Technicon segmented-flow auto-analyzer and using modified colorimetric protocols that allow to achieve a detection limit of 2 nmol L^{-1} (Raimbault et al. 1990; Kerouel and Aminot 1997).

Chl a and primary production—At each station, water samples from six to seven depths in the upper 200 m of the water column were collected for the determination of Chl *a* and primary production. Sampling depths were chosen after examining the irradiance and fluorescence profiles. Chl *a* concentration was measured on board after filtration of 250-mL samples onto $0.2\text{-}\mu\text{m}$ -pore-size polycarbonate filters. Samples were extracted for 12 h in 90% acetone at 4°C overnight. Fluorescence was measured with a Turner Designs 700 fluorometer, which had been calibrated with pure Chl *a*. Primary production was measured with the ^{14}C -uptake technique during on-deck incubations as described in Marañón et al. (2001). For each depth, 75-mL polystyrene bottles (3 light and 1 dark bottles) were filled with seawater just before dawn and spiked with $15 \mu\text{Ci}$ (555 kBq) of $\text{NaH}^{14}\text{CO}_3$. Samples were incubated from dawn to dusk in on-deck flow-through incubators provided with neutral density and blue (Lee Mist Blue) filters that simulated the PAR levels experienced by the phytoplankton in their natural location within the water column. The incubators were refrigerated with running seawater pumped from the surface (for the samples from the upper mixed layer) or with water circulating through a refrigerator (for the samples collected below the upper mixed layer). This system ensured that all water samples were incubated at a temperature within 1.5°C of the in situ

temperature. After the incubation, samples were filtered through 0.2- μm -pore-size polycarbonate filters under low vacuum pressure (< 50 mm Hg). Filters were exposed to concentrated HCl fumes for 10 h in order to remove inorganic ¹⁴C. Finally, liquid scintillation cocktail was added to the filters and the radioactivity present on each sample was measured on a Wallac scintillation counter. For the calculation of carbon fixation rates, the radioactivity measured on the dark samples was subtracted from that measured in the light bottles.

Nitrogen fixation—N₂ fixation was measured at three depths (surface, deep chlorophyll maximum, and an intermediate depth between both) following the ¹⁵N₂ uptake technique described by Montoya et al. (1996). For each depth, three acid-washed, clear polycarbonate bottle (2 liters in volume) were filled directly from the CTD-rosette and supplemented with 2 mL of ¹⁵N₂ (98 atom%; SerCon). Samples were incubated on deck at their original irradiance and temperature conditions during 24 h. After the incubation the whole volume was filtered through a 25-mm GF/F filter (Whatman). Afterward, filters were dried at 40°C for 24 h and then stored until pelletization in tin capsules. ¹⁵N atom% in particulate organic matter was measured with an elemental analyzer combined with a continuous-flow stable isotope mass-spectrometer (Flash-EA112 + Deltaplus; ThermoFinnigan), using an acetanilide standard as reference. The equations given in Weiss (1970) and Montoya et al. (1996) were used to calculate the initial N₂ concentration and N₂ fixation rates, respectively.

Trichodesmium abundance—The ship's underway continuous water supply was used to sample with high spatial resolution (each ~ 60 km) for the determination of surface *Trichodesmium* abundance. After filtering ~ 80 liters (60–105 liters) of seawater through a 40- μm nylon mesh, particles were transferred to a 100-mL glass bottle and preserved in Lugol solution. Back in the laboratory, samples were allowed to settle in sedimentation chambers following the Utermöhl method (Utermöhl 1958) and counting of trichomes was carried out with a Nikon Diaphot microscope. We examined regularly under the microscope fresh samples collected both with the underway water supply system and with Niskin bottles at station, and found that the filaments' shape and length were similar. We did not find broken or damaged filaments in the samples from the continuous water supply system. These observations suggested that our sampling method resulted in reliable estimates of *Trichodesmium* spp. filament abundance. This was later confirmed when we compared our results with those reported by other studies in the same region (Fernández et al. 2010). A complete description of the latitudinal distribution of *Trichodesmium* spp. filament abundance, at high spatial resolution, is included in Fernández et al. (2010), whereas here we only report on the *Trichodesmium* spp. abundance in the locations where the CTD stations were conducted.

Microstructure turbulence—Measurements of dissipation rates of turbulent kinetic energy (ε) were conducted down

to 200 m in 20 stations (see Fig. 1), by using a microstructure profiler (MSS, ISW Wassermesstechnik; Prandke and Stips 1998). The profiler was equipped with two velocity microstructure shear sensors (type PNS98), a microstructure temperature sensor, a high-precision CTD probe, and also a sensor to measure horizontal acceleration of the profiler. The frequency of data sampling was 1024 Hz. The profiler was carefully balanced to have negative buoyancy in the water column and a sinking velocity of ~ 0.4 – 0.7 m s⁻¹. The shear sensors were calibrated just before the cruise and the sensitivity was checked daily during the data processing. Due to significant turbulence generation close to the ship, data were considered reliable below 10 m. The Brunt–Vaisala frequency (N), was derived from CTD profiles according to the equation

$$N^2 = - \left(\frac{g}{\rho_w} \right) \left(\frac{\partial \rho}{\partial z} \right) (s^{-2}) \quad (1)$$

where g is the acceleration due to gravity (9.8 m s⁻²), ρ_w is seawater density (1025 kg m⁻³), and $\partial \rho / \partial z$ is the vertical potential density gradient. The dissipation rate of the turbulent kinetic energy (ε) and the Brunt–Vaisala frequency (N), were averaged over depth intervals of 1-m length. The computing procedure was carried out with the commercial MSSpro processing software and included the removal of spiky data. First, the power spectrum of shear data was computed in the observed wavenumber range. Then, an iterative procedure was applied to determine the Kolmogorov wavenumber, which represents the upper bound for integrating the shear spectrum. The viscous dissipation rate was calculated for each sensor separately, under the assumption of isotropy at the smallest scales. Assuming a universal form of the shear spectrum, the dissipation rate was corrected for the lost variance below and above the integration limits used (see Prandke et al. [2000] for details). Sets of 5–9 turbulence profiles were taken at each station. Despite ongoing discussions regarding the correct averaging method for microstructure turbulence measurements, we followed Davis (1996) in presenting direct arithmetic averages of ε computed over 1-m intervals. Vertical diffusivity (kz) within a stratified fluid was estimated from Osborn (1980) as

$$kz = e \frac{\varepsilon}{N^2} \quad (2)$$

where e is a mixing efficiency ($e = 0.2$ herein).

Vertical nitrate fluxes into the euphotic layer were calculated from the product of the estimated diffusion coefficients kz and the gradients of nanomolar nitrate concentration across the depth of the euphotic layer (1% PAR), determined using linear interpolation.

Results

Physical, chemical, and biological properties across the transect—The main hydrographical feature across the transect was the equatorial upwelling, whose influence could be detected by the location of the 16°C isotherm

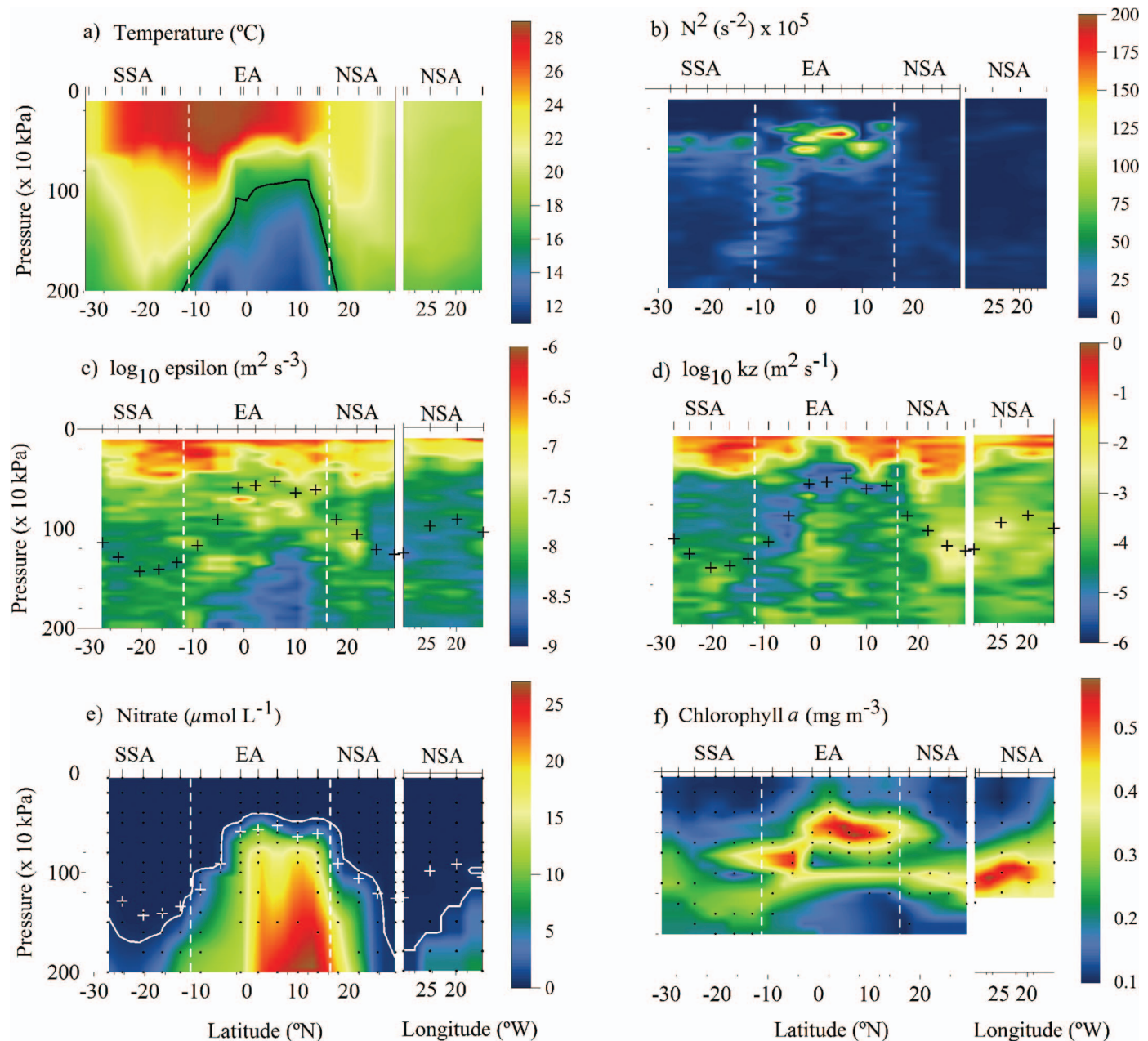


Fig. 2. Vertical distribution of (a) temperature, (b) Brunt Väisälä frequency (N), (c) dissipation rates of turbulent kinetic energy (ϵ), (d) vertical diffusivity (kz), (e) dissolved nitrate, and (f) Chl a concentration during this cruise. Note the logarithm scale for ϵ and kz . Ticks at the top axes correspond to CTD and MST stations. Crosses indicate the base of the euphotic layer. SSA is south subtropical Atlantic, EA is equatorial Atlantic, and NSA is north subtropical Atlantic. Vertical dashed lines indicate the limit between the biogeographic provinces considered in this study. In the temperature and nitrate plots, the 16°C isotherm and $0.5\text{-}\mu\text{mol L}^{-1}$ isoline, respectively, are highlighted.

above 200 m (see Fig. 2a). The depth of this isotherm was used to delimit the three biogeographic provinces that were crossed during this cruise: the south subtropical Atlantic (SSA; $\sim 31^\circ\text{S}$ – 12°S); the equatorial Atlantic (EA; $\sim 12^\circ\text{S}$ – 16°N), where the 16°C isotherm was located above 200 m and that corresponded to the equatorial upwelling region; and the north subtropical Atlantic (NSA; $\sim 16^\circ\text{N}$ – 29°N).

Seasonality and the equatorial upwelling were the main factors controlling the observed pattern in surface stratification, which is illustrated by the distribution of the Brunt

Väisälä frequency (Fig. 2b). The SSA was characterized by warm and stratified surface waters. In this region mean values of Brunt Väisälä frequency in the upper 150 m were $\sim 1.1 \times 10^{-4} \text{ s}^{-2}$ (see Table 1 and Fig. 3a). Due to the uplifting of isotherms and isohalines, the EA was characterized by high vertical stability in the upper 150 m, with mean values of Brunt Väisälä frequency reaching $\sim 2.6 \times 10^{-4} \text{ s}^{-2}$. The NSA, in the North Hemisphere, was characterized by relatively well-mixed waters, with mean values of Brunt Väisälä frequency of $\sim 0.3 \times 10^{-4} \text{ s}^{-2}$.

Table 1. Mean values for selected variables in the three provinces (SSA, EA, and NSA) investigated during this cruise. BVF is Brunt Väisälä frequency averaged over the upper 150 m. The dissipation rate of turbulent kinetic energy (ϵ), vertical diffusivity (kz), nitrate gradient (ΔNO_3), and diffusive nitrate flux were computed at the base of the euphotic zone. Nutricline depth corresponds to the depth of the 0.5 $\mu\text{mol L}^{-1}$ isoline. Chl *a* concentration, primary production (¹⁴C PP), and N₂ fixation rates were integrated down to the base of the euphotic layer. Contribution (%) of N₂ fixation to total new nitrogen input is indicated. A nonparametric one-way analysis of variance (Kruskall–Wallis) was performed to test the null hypothesis that independent different groups come from distributions with equal medians. SD is standard deviation, *p* is statistical probability, *n* is number of stations, and *m* number of MSS profiles. Mean values for ϵ , kz is diffusive nitrate flux, and contribution of N₂ fixation include the variability among all the MSS profiles deployed in each province. The Bonferroni multiple-comparison test was applied a posteriori to analyze the differences between every pair of groups. Statistically significance at level $\alpha = 0.05$ (*) and $\alpha = 0.01$ (**) is indicated.

Variable (units)	(1) SSA† 31°S–12°S (mean ± SD)	(2) EA‡ 12°S–16°N (mean ± SD)	(3) NSA§ ~16°N–29°N (mean ± SD)	Kruskall– Wallis <i>p</i>	Bonferroni comparisons
Surface temperature (°C)	26 ± 2	28 ± 2	21 ± 1	0.002**	3 < 2
16°C isotherm depth (m)	234 ± 25	113 ± 34	172 ± 23	0.001**	2 < 1, 3
BVF (s ⁻²) × 10 ⁻⁴	1.1 ± 0.1	2.6 ± 0.5	0.3 ± 0.3	0.0002**	2 > 3
ϵ (m ² s ⁻³) × 10 ⁻⁸	0.6 ± 0.4	2 ± 3	1 ± 1	0.002**	2 > 1, 3
Vertical diffusivity (m ² s ⁻¹) × 10 ⁻⁴	0.5 ± 0.5	0.1 ± 0.2	5 ± 7	< 0.001**	3 > 1 > 2
ΔNO_3 ($\mu\text{mol N m}^{-4}$)	7 ± 8	495 ± 357	62 ± 90	0.003**	2 > 1
Nutricline depth (m)	158 ± 12	64 ± 31	128 ± 36	0.003**	2 < 1
NO ₃ flux ($\mu\text{mol N m}^{-2} \text{d}^{-1}$)	34 ± 50	405 ± 888	844 ± 1258	< 0.001**	1 < 2, 3
Surface chlorophyll <i>a</i> (mg m ⁻³)	0.12 ± 0.02	0.18 ± 0.04	0.14 ± 0.03	0.012*	1 < 2
Total chlorophyll <i>a</i> (mg m ⁻²)	25 ± 3	25 ± 3	22 ± 2	0.054	
¹⁴ C PP (mmol C m ⁻² d ⁻¹)	8 ± 2	19 ± 8	15 ± 5	0.012*	1 < 2, 3
Surface <i>Trichodesmium</i> abundance (trichomes L ⁻¹)	1 ± 1	162 ± 97	6 ± 8	0.002**	2 > 1, 3
N ₂ fixation ($\mu\text{mol N m}^{-2} \text{d}^{-1}$)	10 ± 10	56 ± 49	11 ± 9	0.027*	2 > 3
% N ₂ fixation	44 ± 30	22 ± 19	2 ± 2	< 0.001**	1 > 2 > 3

† *n* = 6, *m* = 33.

‡ *n* = 7, *m* = 38.

§ *n* = 7, *m* = 42.

Hydrographical properties in the last part of the cruise (west–east transect) were influenced by the coastal North African upwelling.

As a consequence of wind forcing at the atmosphere–ocean interface, maximum values of dissipation rates of turbulent kinetic energy (ϵ) were measured at the surface layer (Fig. 2c). The base of the euphotic zone, which was located deeper at the SSA (~ 135 m) compared with the NSA (~ 106 m) and the EA (~ 85 m), was associated with lower values of ϵ in the SSA (0.6 ± 0.4) compared to the NSA (1 ± 1) and the EA (2 ± 3 ; see Table 1 and Fig. 3b). The magnitude of vertical diffusivity (kz) computed along the transect (Fig. 2d) was the result of the described stratification conditions and the distribution of ϵ (see Methods). Maximum values were computed at the surface, whereas diffusivity was lower in those regions characterized by intense stratification. The base of the euphotic zone was associated with relative high values of diffusivity in the NSA ($5 \times 10^{-4} \pm 7 \times 10^{-4} \text{ m}^2 \text{ s}^{-1}$), whereas the SSA ($0.5 \times 10^{-4} \pm 0.5 \times 10^{-4} \text{ m}^2 \text{ s}^{-1}$) and the EA ($0.1 \times 10^{-4} \pm 0.2 \times 10^{-4} \text{ m}^2 \text{ s}^{-1}$) were characterized by lower values (see Table 1 and Fig. 3c).

The main signature in the nitrate distribution along the transect was the influence of the equatorial upwelling (Fig. 2e). The nutricline was quite deep (158 ± 12 m) in the SSA, uplifted in the EA (64 ± 31 m) and went deep again in the NSA (128 ± 36 m; Table 1). Nitrate gradient computed across the base of the euphotic layer was higher in the EA ($495 \pm 357 \mu\text{mol N m}^{-4}$) compared to the SSA ($7 \pm 8 \mu\text{mol N m}^{-4}$) and the NSA ($62 \pm 90 \mu\text{mol N m}^{-4}$; see Fig. 3d).

The vertical distribution of Chl *a* concentration was characterized, in general, by low values ($< 0.15 \text{ mg m}^{-3}$) at the surface and the presence of a deep chlorophyll maximum (DCM; Fig. 2f). Surface Chl *a* was enhanced in the EA (~ 0.18 mg m⁻³) and in the waters close to the African coast (see also Fig. 3e). The DCM that was located deep in the SSA (at ~ 135 m) uplifted up to ~ 85 m in the EA. In the NSA, although the nutricline and the chlorophyll maximum (~ 106 m) uplifted in the waters close to the African coast, both were located deeper compared to EA.

No large differences among regions were found in total Chl *a* integrated down to the base of the euphotic layer. Maximum values of total primary production were measured in EA ($19 \pm 8 \text{ mmol C m}^{-2} \text{ d}^{-1}$), whereas the minimum rates were associated with the warm and stratified waters of SSA ($8 \pm 2 \text{ mmol C m}^{-2} \text{ d}^{-1}$; see Table 1 and Fig. 3f).

Contribution of N₂ fixation to total new nitrogen input—The comparison of N₂ fixation vs. nitrate eddy diffusion, and the contribution of N₂ fixation to total new nitrogen input (N₂ fixation + nitrate diffusion) are shown in Fig. 1. N₂ fixation rates were detectable in all the stations and ranged from a minimum value of 1.3 $\mu\text{mol N m}^{-2} \text{ d}^{-1}$ at 29.2°N (NSA) up to 154.5 $\mu\text{mol N m}^{-2} \text{ d}^{-1}$ at 2.2°N (EA). The mean value for EA was $56 \pm 49 \mu\text{mol N m}^{-2} \text{ d}^{-1}$, whereas SSA and NSA were characterized by lower, and

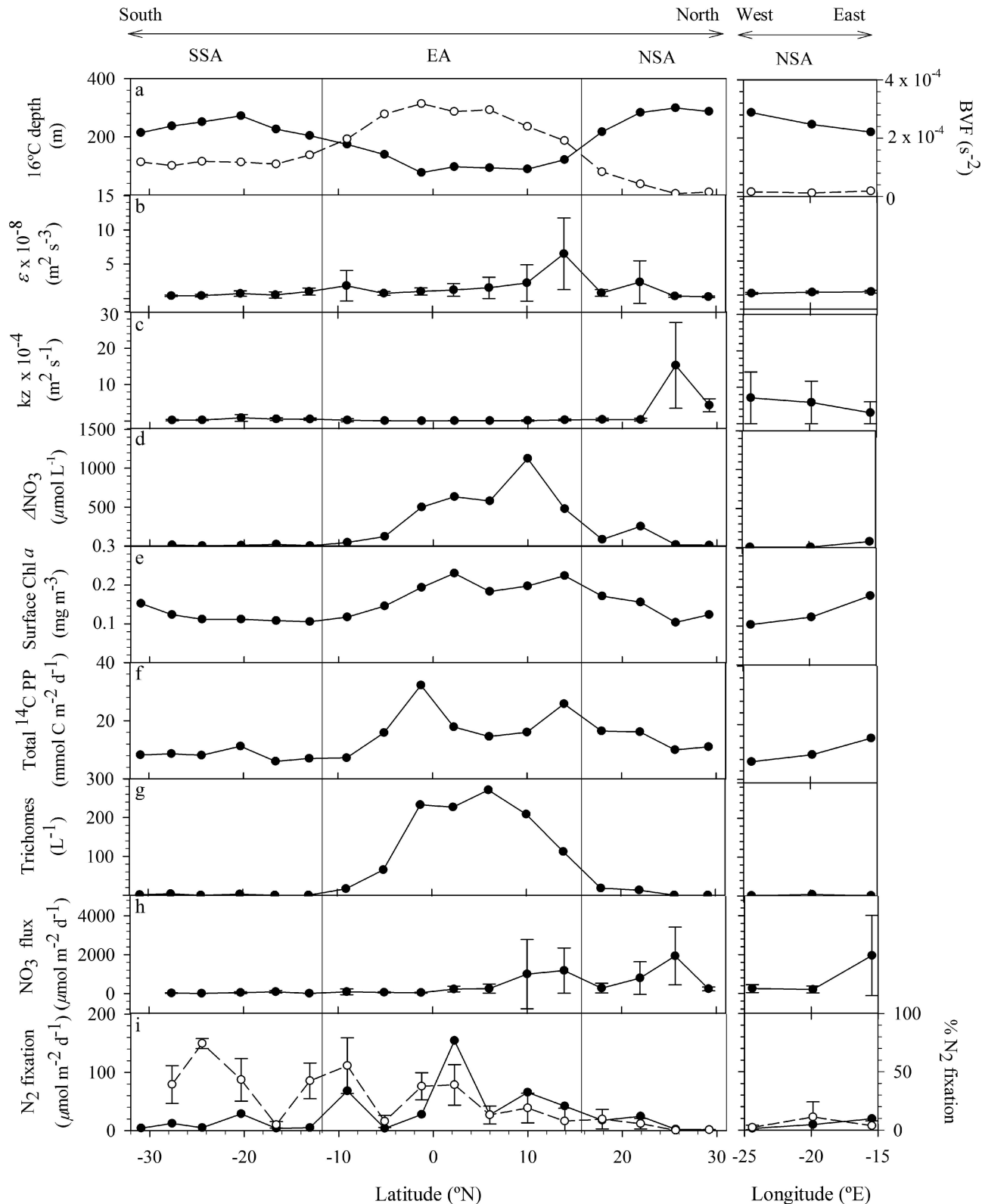


Fig. 3. Latitudinal and longitudinal variability in (a) depth of the 16°C isotherm and Brunt Väisälä frequency (BVF) averaged in the upper 150 m; (b) dissipation rates of turbulent kinetic energy (ϵ), (c) vertical diffusivity (kz), (d) nitrate gradient, and (h) nitrate diffusive flux computed across the base of the euphotic layer; (e) surface chlorophyll *a* (Chl *a*); (f) primary production (^{14}C PP); (g) *Trichodesmium* abundance; (i) N_2 fixation and contribution of N_2 fixation to the total inputs of new nitrogen into the euphotic layer during this cruise. SSA is the south subtropical Atlantic, EA is the equatorial Atlantic, and NSA is the north subtropical Atlantic. Error bars associated with ϵ , diffusivity, nitrate diffusive fluxes, and the contribution of N_2 fixation to the total inputs of new nitrogen correspond to standard deviations and derived from the variability of the 5–9 turbulence profiles taken at each station (see Methods).

similar values of $\sim 10 \mu\text{mol N m}^{-2} \text{d}^{-1}$ (Table 1). A slight increase in N₂ fixation was observed from the open ocean ($1.3 \mu\text{mol N m}^{-2} \text{d}^{-1}$) to the African coast ($19.5 \mu\text{mol N m}^{-2} \text{d}^{-1}$) along the 29°N west–east transect.

Nitrate eddy diffusion ranged from a minimum value of $0.6 \pm 0.3 \mu\text{mol m}^{-2} \text{d}^{-1}$ at 24.4°S (SSA) up to $1950 \pm 2064 \mu\text{mol m}^{-2} \text{d}^{-1}$ at 29.2°N (NSA; Fig. 1b). Nitrate supply through eddy diffusion depended on mixing conditions and the nitrate gradient at the base of the euphotic zone (see Methods). In the EA, the sharp nitrate gradient due to the isolines uplifting compensated for the low diffusivity. As a result, nitrate eddy diffusion accounted for $405 \pm 888 \mu\text{mol N m}^{-2} \text{d}^{-1}$, so the contribution of N₂ fixation to total new nitrogen input was $22\% \pm 19\%$ (see Table 1 and Fig. 3h,i). Although SSA and NSA were very similar in terms of N₂ fixation rates, they exhibited statistically significant differences ($p < 0.001$) in the magnitude of nitrate eddy diffusion. The low diffusivity and low nitrate gradient found in SSA resulted in an eddy diffusive flux of nitrate of $34 \pm 50 \mu\text{mol N m}^{-2} \text{d}^{-1}$. This value is one order of magnitude lower than the value computed for NSA ($844 \pm 1258 \mu\text{mol N m}^{-2} \text{d}^{-1}$), which was the result of the higher diffusivity and nitrate gradient measured in this region. As a consequence of the asymmetry in diffusive fluxes, the contribution of N₂ fixation to new nitrogen input in SSA was $44\% \pm 30\%$, whereas this process only represented $2\% \pm 2\%$ of the new nitrogen entering the euphotic zone in NSA.

The distribution of surface *Trichodesmium* abundance was consistent with the observed distribution of N₂ fixation rates, with significantly higher abundances being found in EA (162 ± 97 filaments L⁻¹; see Table 1 and Fig. 3g). Although SSA and NSA had similar mean rates of N₂ fixation, *Trichodesmium* abundance was lower in SSA (1 ± 1 trichome L⁻¹) compared to NSA (6 ± 8 trichome L⁻¹).

Discussion

Primary production rates measured during this cruise are consistent with the range of variability in primary production reported for the Atlantic subtropical regions during previous latitudinal transects (Marañón et al. 2000; Poulton et al. 2006). The N₂ fixation rates we measured are in the same range as those reported by Moore et al. (2009), which peaked between $\sim 5^\circ\text{N}$ and 15°N at $\sim 200 \mu\text{mol m}^{-2} \text{d}^{-1}$. The pattern of surface *Trichodesmium* abundance described during this cruise is also in agreement with that observed previously in the Atlantic, which revealed a very consistent pattern of higher densities (300 ± 101 trichomes L⁻¹) in the region between 0°N and $\sim 15^\circ\text{N}$ (Tyrrell et al. 2003; Moore et al. 2009). The observation that, despite the similar values of N₂ fixation, *Trichodesmium* abundance was lower in SSA compared to NSA suggest a higher contribution of unicellular nitrogen fixers in SSA (Montoya et al. 2007). The assessment of the relative importance of different environmental factors, such as dust deposition, phosphorus availability, and water column structure, in determining the large-scale variability of *Trichodesmium* spp. abundance and community N₂ fixation during this cruise and another contrasting season is presented in Fernández et al. (2010).

Recently, it has been shown that the ¹⁵N₂-tracer-addition method underestimates N₂ fixation rates significantly when the ¹⁵N₂ tracer is introduced as a gas bubble that does not attain equilibrium with the surrounding waters (Mohr et al. 2010). However, according to these authors the evaluation of the underestimation is not straightforward because it varies with the incubation time, the amount of injected gas and the timing of the bubble injection relative to diel N₂ fixation patterns. We used long (24-h) incubations, which would have resulted in a lower underestimation than if we had used shorter incubations. If our N₂ fixation rates are underestimates, we are also underestimating the contribution of this process vs. nitrate diffusion as a source of new nitrogen in the Atlantic Ocean. Importantly, there is no evidence to suggest that the underestimation of N₂ fixation by the N₂-uptake technique, as used conventionally, is systematically larger in any given region of the ocean. This means that, to a first order, the latitudinal patterns we describe remain valid, even if the absolute rates we report are somewhat underestimated.

Planas et al. (1999) used the empirical parameterization proposed by Gregg (1989) to compute diffusivity across a similar transect carried out in March–April 1995. Except for the EA, these authors reported diffusivity values that were about one order of magnitude lower than our estimates. This difference was compensated by higher nitrate gradients computed at the thermocline, which resulted in nitrate diffusive fluxes ($\sim 13 \mu\text{mol N m}^{-2} \text{d}^{-1}$, $612 \mu\text{mol N m}^{-2} \text{d}^{-1}$, and $743 \mu\text{mol N m}^{-2} \text{d}^{-1}$, for the SSA, the EA, and the NSA; respectively) that were in agreement with our estimates.

Differences in nitrate diffusion observed during this cruise spanned more than one order of magnitude; however, phytoplankton carbon-fixation rates measured in NSA ($15 \pm 5 \text{ mg C m}^{-2} \text{h}^{-1}$) were only twice the values found in SSA ($8 \pm 2 \text{ mg C m}^{-2} \text{h}^{-1}$). Assuming mean values for the percentage of dissolved organic carbon production with respect to total integrated primary production ($\sim 23\%$; Teira et al. 2001), the ratio of phytoplankton respiration to gross photosynthesis ($\sim 20\%$; Geider 1992), and the Redfield stoichiometry for carbon and nitrogen, we computed mean values for total (dissolved plus particulate) gross primary production in SSA and NSA of $1.7 \text{ mmol N m}^{-2} \text{d}^{-1}$ and $3.3 \text{ mmol N m}^{-2} \text{d}^{-1}$, respectively. The total amount of new nitrogen entering the euphotic zone (N₂ fixation plus nitrate diffusion) compared to these estimates of total gross primary production reveals a remarkable asymmetry in the value of the *f*-ratio for SSA (~ 0.02) and NSA (~ 0.24). This asymmetry is consistent with maps of annual particulate-matter export calculated from satellite color data describing lower export rates in SSA (Dunne et al. 2005), and with *f*-ratio estimates that include the effect of surface nitrification (Yool et al. 2007). Additional sources of nitrogen, not considered in this study, could compensate the observed asymmetry in the *f*-ratio values computed for SSA and NSA. Model results indicate that atmospheric deposition of anthropogenic nitrogen is rapidly approaching the same order of magnitude as ocean N₂ fixation (Duce et al. 2008). However, according to these authors,

the magnitude of this process is about the same in SSA and NSA ($\sim 15 \mu\text{mol N m}^{-2} \text{d}^{-1}$). Unfortunately, the limited temporal and spatial resolution of our sampling design does not allow us to investigate the contribution of additional nitrogen sources as episodic nutrient injections associated with sub- and mesoscale turbulence (McGillicuddy and Robinson 1998; Oschlies and Garçon 1998) or lateral transport of inorganic and organic nutrients (Williams and Follows 1998; Torres-Valdes et al. 2009). Due to the influence of the coastal North African upwelling, lateral transport of nutrients is expected to be more important in NSA. Therefore, the consideration of this mechanism would intensify the asymmetry between NSA and SSA in the f -ratio value. The differences we have observed between SSA and NSA were due, in part, to differences in the contrasting seasonal forcing affecting each hemisphere at the time of the cruise. The comparison of community N_2 fixation rates along the same meridional transect during two contrasting seasons, October–November 2007 and April–May 2008, reported in Fernández et al. (2010), indicates that higher N_2 fixation rates were measured in each hemisphere after the period characterized by strong seasonal thermal stratification. N_2 fixation rates in the NSA were higher in October–November ($25 \pm 6 \mu\text{mol N m}^{-2} \text{d}^{-1}$) than in April–May ($11 \pm 4 \mu\text{mol N m}^{-2} \text{d}^{-1}$), whereas the opposite trend was found in the SSA ($3 \pm 1 \mu\text{mol N m}^{-2} \text{d}^{-1}$ vs. $10 \pm 2 \mu\text{mol N m}^{-2} \text{d}^{-1}$ in Apr–May). The high nitrate diffusive fluxes computed in NSA in April–May were mainly due to the high diffusivity ($\sim 5 \times 10^{-4} \text{m}^2 \text{s}^{-1}$) that characterized the well-mixed waters in this region and time of the year (see Fig. 3). In the last station that was occupied during this cruise, where the influence of the coastal North African upwelling was noticeable, high nitrate fluxes were also due to a relatively higher nitrate gradient across the base of the euphotic zone. The comparative analysis of hydrography data obtained in October–November 2007 and April–May 2008 showed that the influence of the African upwelling in this region also has a seasonal component (data not shown). Unfortunately, because measurements of ε were not taken in October–November 2007, we cannot compare (at least by using the same methodology) the contribution of N_2 fixation to the new N in this contrasting season. However, although the differences between SSA and NSA in the contribution of N_2 fixation may be lower in other seasons, our results still indicate a large spatial variability in biogeochemical cycling that is uncoupled from the relative constant biomass standing stocks.

Our study reveals striking differences in the nitrogen budgets of the south and north subtropical gyres. In spite of similar phytoplankton standing stocks and relatively small differences in primary production, the two regions differed greatly in the dominant sources of new nitrogen, the estimated f -ratio and their potential for organic carbon export. The accurate determination of diffusivity, conducted for the first time across a basin-scale transect, showed a large degree of spatial variability in nitrate supply through eddy diffusion into the euphotic zone. This variability resulted in statistically significant differences between SSA and NSA ($p < 0.001$, see Table 1) in the contribution of N_2 fixation to the new nitrogen input. Although turbulent dissipation in the oceans is highly heterogeneous and

intermittent, our results show that at the time of this cruise the differences between the north and south subtropical Atlantic were higher than the differences among all the profiles taken in each province (see Fig. 3). This result evidences the relevance of considering the variability in diffusivity, vs. assuming constant coefficients, when estimating the budget of nitrogen inputs into the surface layer of subtropical regions (Capone et al. 2005).

The limited data available so far (Moore et al. 2009), suggest that N_2 fixation can be considered unimportant in the south subtropical Atlantic. However, the low rates found in this region can explain $> 40\%$ of the new nitrogen entering the euphotic zone, at least during a period of enhanced thermal stratification. The predicted effects of global change scenarios include warming of the surface ocean and the expansion of the oligotrophic, subtropical regions (Polovina et al. 2008). As the oceans become more strongly stratified, it is expected that the vertical diffusion of nitrate will weaken and, therefore, that N_2 fixation will become more relevant as a source of new nitrogen. Understanding the spatial and temporal heterogeneities in the mechanisms controlling nutrient supply (Mather et al. 2008) is crucial to predict the response of the biological pump to long-term changes in the Earth system.

Acknowledgments

We thank the officers and crew of the R/V *Hespérides*, as well as the staff of the Marine Technology Unit, for their support during the work at sea. We also thank X. Irigoien (AZTI-Tecnalia) and H. Prandke for logistic and technical support with the microstructure profiler, and J. García and F. Eiroa for microscope counting of trichomes. Comments by two anonymous reviewers have improved a previous version of the manuscript.

This work was funded by the Spanish Ministry of Education and Science through grants CTM2004-05174-C02 (*Trichodesmium* and N_2 fixation in the tropical Atlantic) to E. Marañón and CTM2007-28925- E/MAR (Turbulence along a latitudinal transect in the tropical Atlantic) to B. Mouriño. B. Mouriño was supported by the I. Parga-Pondal program from the Galician government.

References

- CAPONE, D. G., AND OTHERS. 2005. Nitrogen fixation by *Trichodesmium* spp.: An important source of new nitrogen to the tropical and subtropical North Atlantic Ocean. *Glob. Biogeochem. Cycles* **19**: GB2024, doi:10.1029/2004GB002331
- DAVIS, R. E. 1996. Sampling turbulent dissipation. *J. Phys. Oceanogr.* **26**: 341–358, doi:10.1175/1520-0485(1996)026<0341:STD>2.0.CO;2
- DUCE, R. A., AND OTHERS. 2008. Impacts of atmospheric anthropogenic nitrogen on the open ocean. *Science* **320**: 893–897, doi:10.1126/science.1150369
- DUNNE, J. P., R. A. ARMSTRONG, A. GNANADESIKAN, AND J. L. SARMIENTO. 2005. Empirical and mechanistic models for the particle export ratio. *Glob. Biogeochem. Cycles* **19**: GB4026, doi:10.1029/2004GB002390
- EMERSON, S., P. QUAY, D. KARL, C. WINN, L. TUPAS, AND M. LANDRY. 1997. Experimental determination of the organic carbon flux from open-ocean surface waters. *Nature* **389**: 951–954, doi:10.1038/40111
- EPPLEY, R. W., AND B. J. PETERSON. 1979. Particulate organic matter flux and planktonic new production in the deep ocean. *Nature* **282**: 677–680, doi:10.1038/282677a0

- FALKOWSKI, P. G. 1997. Evolution of nitrogen cycle and its influence on the biological pump in the ocean. *Nature* **342**: 637–642, doi:10.1038/387272a0
- FERNÁNDEZ, A., B. MOURIÑO-CARBALLIDO, A. BODE, M. VARELA, AND E. MARAÑÓN. 2010. Latitudinal distribution of *Trichodesmium* spp. and N₂ fixation in the Atlantic Ocean. *Biogeosciences* **7**: 3167–3176, doi:10.5194/bg-7-3167-2010
- GEIDER, R. J. 1992. Respiration: Taxation without representation?, p. 333–360. In P. G. Falkowski and A. D. Woodhead [eds.], *Primary productivity and biogeochemical cycles in the sea*. Plenum Press.
- GREGG, M. C. 1989. Scaling turbulent dissipation in the thermocline. *J. Geophys. Res.-Oceans* **94**: 9686–9698, doi:10.1029/JC094iC07p09686
- KATIJA, K., AND J. O. DABIRI. 2009. A viscosity-enhanced mechanism for biogenic ocean mixing. *Nature* **460**: 624–U687, doi:10.1038/nature08207
- KEROUEL, R., AND A. AMINOT. 1997. Fluorometric determination of ammonia in sea and estuarine waters by direct segmented flow analysis. *Mar. Chem.* **57**: 265–275, doi:10.1016/S0304-4203(97)00040-6
- LEDWELL, J. R., A. J. WATSON, AND C. S. LAW. 1993. Evidence for slow mixing across the pycnocline from an open-ocean tracer-release experiment. *Nature* **364**: 701–703, doi:10.1038/364701a0
- LEWIS, M. R., W. G. HARRISON, N. S. OAKELY, D. HEBERT, AND T. PLATT. 1986. Vertical nitrate fluxes in the oligotrophic ocean. *Science* **234**: 870–873, doi:10.1126/science.234.4778.870
- MARAÑÓN, E., P. M. HOLLIGAN, R. BARCIELA, N. GONZALEZ, B. MOURINO, M. J. PAZO, AND M. VARELA. 2001. Patterns of phytoplankton size structure and productivity in contrasting open-ocean environments. *Mar. Ecol.-Prog. Ser.* **216**: 43–56, doi:10.3354/meps216043
- , M. VARELA, B. MOURINO, AND A. J. BALE. 2000. Basin-scale variability of phytoplankton biomass, production and growth in the Atlantic Ocean. *Deep-Sea Res. Part I* **47**: 825–857, doi:10.1016/S0967-0637(99)00087-4
- MATHER, R. L., AND OTHERS. 2008. Phosphorus cycling in the North and South Atlantic Ocean subtropical gyres. *Nat. Geosci.* **1**: 439–443, doi:10.1038/ngeo232
- MCGILLICUDDY, D. J., AND A. R. ROBINSON. 1998. Interaction between the oceanic mesoscale and the surface mixed layer. *Dyn. Atmos. Oceans* **27**: 549–574, doi:10.1016/S0377-0265(97)00030-4
- MOHR, W., T. GROSSKOPF, D. W. R. WALLACE, AND J. LAROCHE. 2010. Methodological underestimation of oceanic nitrogen fixation rates. *PLoS One* **5**: e12583, doi:10.1371/journal.pone.0012583
- MONTOYA, J. P., M. VOSS, AND D. G. CAPONE. 2007. Spatial variation in N₂-fixation rate and diazotroph activity in the Tropical Atlantic. *Biogeosciences* **4**: 369–376, doi:10.5194/bg-4-369-2007
- , P. KAHLER, AND D. G. CAPONE. 1996. A simple, high-precision, high-sensitivity tracer assay for N₂ fixation. *Appl. Environ. Microbiol.* **62**: 986–993.
- MOORE, C. M., AND OTHERS. 2009. Large-scale distribution of Atlantic nitrogen fixation controlled by iron availability. *Nat. Geosci.* **2**: 867–871, doi:10.1038/ngeo667
- MUNK, W. 1966. Abyssal recipes. *Deep-Sea Res.* **13**: 713–730.
- NAJJAR, R. G., AND OTHERS. 2007. Impact of circulation on export production, dissolved organic matter, and dissolved oxygen in the ocean: Results from Phase II of the Ocean Carbon-cycle Model Intercomparison Project (OCMIP-2). *Glob. Biogeochem. Cycles* **21**: GB3007, doi:10.1029/2006GB002857
- OSBORN, T. R. 1980. Estimates of the local rate of vertical diffusion from dissipation measurements. *J. Phys. Oceanogr.* **10**: 83–89, doi:10.1175/1520-0485(1980)010<0083:EOTLRO>2.0.CO;2
- OSCHLIES, A., AND V. GARCON. 1998. Eddy-induced enhancement of primary production in a model of the North Atlantic Ocean. *Nature* **394**: 266–269, doi:10.1038/28373
- PLANAS, D., S. AGUSTI, C. M. DUARTE, T. C. GRANATA, AND M. MERINO. 1999. Nitrate uptake and diffusive nitrate supply in the Central Atlantic. *Limnol. Oceanogr.* **44**: 116–126, doi:10.4319/lo.1999.44.1.0116
- POLOVINA, J. J., E. A. HOWELL, AND M. ABECASSIS. 2008. Oceans least productive waters are expanding. *Geophys. Res. Lett.* **35**: L03618, doi:10.1029/2007GL031745
- POULTON, A. J., AND OTHERS. 2006. Phytoplankton carbon fixation, chlorophyll-biomass and diagnostic pigments in the Atlantic Ocean. *Deep-Sea Res. Part II* **53**: 1593–1610, doi:10.1016/j.dsr2.2006.05.007
- PRANDKE, H., K. HOLTSCH, AND A. STIPS. 2000. MITEC technology development: The microstructure/turbulence measuring system. MSS:Technical report EUR 19733 EN. European Commission.
- , AND A. STIPS. 1998. Test measurements with an operational microstructure-turbulence profiler: Detection limit of dissipation rates. *Aquat. Sci.* **60**: 191–209, doi:10.1007/s000270050036
- RAIMBAULT, P., G. SLAWYK, AND V. GENTILHOMME. 1990. Direct measurements of nanomolar nitrate uptake by the marine diatom *Phaeodactylum tricornutum* (Bohlin). Implications for studies of oligotrophic ecosystems. *Hydrobiologia* **207**: 311–318, doi:10.1007/BF00041470
- SRIVER, R. L., AND M. HUBER. 2007. Observational evidence for an ocean heat pump induced by tropical cyclones. *Nature* **447**: 577–580, doi:10.1038/nature05785
- TEIRA, E., M. J. PAZO, P. SERRET, AND E. FERNANDEZ. 2001. Dissolved organic carbon production by microbial populations in the Atlantic Ocean. *Limnol. Oceanogr.* **46**: 1370–1377, doi:10.4319/lo.2001.46.6.1370
- TORRES-VALDES, S., AND OTHERS. 2009. Distribution of dissolved organic nutrients and their effect on export production over the Atlantic Ocean. *Glob. Biogeochem. Cycles* **23**: GB4019, doi:10.1029/2008GB003389
- TYRRELL, T., E. MARANON, A. J. POULTON, A. R. BOWIE, D. S. HARBOUR, AND E. M. S. WOODWARD. 2003. Large-scale latitudinal distribution of *Trichodesmium* spp. in the Atlantic Ocean. *J. Plankton Res.* **25**: 405–416, doi:10.1093/plankt/25.4.405
- UTERMÖHL. 1958. Zur vervollkommnung der quantative phytoplankton-methodik. *Mitteilungen aus Institut Verhein Limnologie* **9**: 1–38. [For perfection of the quantitative phytoplankton methodology.]
- WEISS, R. F. 1970. Solubility of nitrogen, oxygen and argon in water and seawater. *Deep-Sea Res.* **17**: 721–735.
- WILLIAMS, R. G., AND M. J. FOLLOWS. 1998. The Ekman transfer of nutrients and maintenance of new production over the North Atlantic. *Deep-Sea Res. Part I* **45**: 461–489, doi:10.1016/S0967-0637(97)00094-0
- WUNSCH, C., AND R. FERRARI. 2004. Vertical mixing, energy and the general circulation of the oceans. *Ann. Rev. Fluid Mech.* **36**: 281–314, doi:10.1146/annurev.fluid.36.050802.122121
- YOOL, A., A. P. MARTIN, C. FERNANDEZ, AND D. R. CLARK. 2007. The significance of nitrification for oceanic new production. *Nature* **447**: 999–1002, doi:10.1038/nature05885

Associate editor: Mary I. Scranton

Received: 14 September 2010

Accepted: 13 January 2011

Amended: 08 February 2011